TOXICOLOGICAL SCIENCES **112(2)**, 521–531 (2009)
doi:10.1093/toxsci/kfp235
Advance Access publication September 25, 2009

High-Mobility Group Box-1 Protein and Keratin-18, Circulating Serum Proteins Informative of Acetaminophen-Induced Necrosis and Apoptosis *In Vivo*

Daniel J. Antoine,*[,1] Dominic P. Williams,* Anja Kipar,† Rosalind E. Jenkins,* Sophie L. Regan,* Jean G. Sathish,* Neil R. Kitteringham,* and B. Kevin Park*

**MRC Centre for Drug Safety Science, Department of Pharmacology & Therapeutics; and †MRC Centre for Drug Safety Science, Department of Veterinary Pathology, Faculty of Veterinary Science, University of Liverpool, Liverpool L69 3GE, UK*

Received July 31, 2009; accepted September 17, 2009

Drug-induced hepatotoxicity represents a major clinical problem and an impediment to new medicine development. Serum biomarkers hold the potential to provide information about pathways leading to cellular responses within inaccessible tissues, which can inform the medicinal chemist and the clinician with respect to safe drug design and use. Hepatocyte apoptosis, necrosis, and innate immune activation have been defined as features of the toxicological response associated with the hepatotoxin acetaminophen (APAP). Within this investigation, we have unambiguously identified and characterized by liquid chromatography-tandem mass spectrometry differing circulating molecular forms of high-mobility group box-1 protein (HMGB1) and keratin-18 (K18), which are linked to the mechanisms and pathological changes induced by APAP in the mouse. Hypoacetylated HMGB1 (necrosis indicator), caspase-cleaved K18 (apoptosis indicator), and full-length K18 (necrosis indicator) present in serum showed strong correlations with the histological time course of cell death and was more sensitive than alanine aminotransferase activity. We have further identified a hyperacetylated form of HMGB1 (inflammatory indicator) in serum, which indicated that hepatotoxicity was associated with an inflammatory response. The inhibition of APAP-induced apoptosis and K18 cleavage by the caspase inhibitor N-benzyloxycarbonyl-Val-Ala-Asp(OMe) fluoromethyl ketone are associated with increased hepatic damage, by a shift to necrotic cell death only. These findings illustrate the initial verification of K18 and HMGB1 molecular forms as serum-based sensitive tools that provide insights into the cellular dynamics involved in APAP hepatotoxicity within an inaccessible tissue. Based on these findings, potential exists for the qualification and measurement of these proteins to further assist *in vitro*, *in vivo*, and clinical bridging in toxicological research.

Key Words: **biomarker; bioactivation; caspase; hepatotoxicity; inflammation; ROC.**

Adverse drug reactions (ADRs) are a clinical concern and cause attrition in drug development with hepatotoxicity being a major contributor (Pirmohamed *et al*., 2004). Metabolic activation of drugs is an important mechanism in drug-induced liver injury (DILI) (Park *et al*., 2005). The cellular events that link drug metabolism to clinical outcome are poorly understood. A better understanding of the mechanisms and pathways leading to DILI would improve clinical management and inform the design of safer medicines.

The importance of biomarkers to accelerate the pace of drug development, reduce attrition, and to be biologically informative is generally acknowledged. Selective serum markers of apoptosis, necrosis, and inflammation would have benefit for differentiating the underlying mechanisms of DILI. Acetaminophen (APAP), a hepatotoxin in murine systems and a significant cause of clinical ADRs, can be used to investigate potential informative- and mechanism-based biomarkers of DILI. Biochemical events leading to initiation of APAP hepatotoxicity through cytochrome P450–mediated formation of N-acetyl-*p*-benzo-quinoneimine and subsequent requirement for glutathione (GSH) depletion are well defined (Dahlin *et al*., 1984). Necrosis is the final and ultimate form of cell death. However, several reports suggest that intracellular events following APAP metabolic activation can lead to hepatocyte apoptosis (Kon *et al*., 2007). The extent to which remains controversial (Gujral *et al*., 2002; Gunawan *et al*., 2006).

Keratins are intermediate filament proteins expressed by epithelial cells responsible for cell structure and integrity. Phosphorylation of key serine residues within Keratin-18 (K18) occurs early in Fas-mediated apoptosis (Ku and Omary, 2001). Caspase-mediated cleavage of K18 is an early event in structural rearrangement during apoptosis (Caulin *et al*., 1997). Caspases-3, -7, and-9 have been implicated in the cleavage of K18 at the C-terminal DALD/S motif. Caspase-6 has been shown to cleave at the VEVD/A motif within the L1-2 linker region. Full-length K18 released passively during necrotic cell

[1] To whom correspondence should be addressed at MRC Centre for Drug Safety Science, Department of Pharmacology and Therapeutics, University of Liverpool, Sherrington Buildings, Ashton Street, Liverpool L69 3GE, UK. E-mail: d.antoine@liv.ac.uk.

death and fragmented K18 generated during apoptosis can be released into the blood and accumulate over time (Schutte *et al*., 2004). Antibodies have been raised against apoptosis-related forms of K18 (Cummings *et al*., 2008b; Tao *et al*., 2008). Serum quantification of caspase-cleaved and full-length K18 that can represent markers of apoptosis and necrosis, respectively, have been used during pharmacodynamic chemotherapeutic drug monitoring in patients and animal models (Cummings *et al*., 2008a). K18 has also been employed for the quantification of apoptosis during liver disorders such as nonalcoholic steatohepatitis (Wieckowska *et al*., 2006) and hepatitis C virus infection (Bantel *et al*., 2004).

APAP hepatotoxicity has been associated with the activation of the Nalp3 inflammasome (Imaeda *et al*., 2009) and the innate immune response (Liu *et al*., 2004). Although the overall extent of injury outcome is thought to be dependent upon the balance between proinflammatory and anti-inflammatory signaling of innate immune cells and hepatocytes during APAP hepatotoxicity, controversy still remains (Jaeschke, 2006; Masson *et al*., 2008). Recent evidence suggests a key role played by high-mobility group box-1 (HMGB1) protein in alerting the immune system to dying cells (Kono and Rock, 2008; Scaffidi *et al*., 2002). HMGB1 is a nuclear-binding protein that has proinflammatory activity and targets toll-like receptors and the receptor for advanced glycation end products on target cells (Hori *et al*., 1995; Park *et al*., 2004). It is released in a hyperacetylated form with the involvement of distinct lysine residues from activated innate immune cells (Bonaldi *et al*., 2003) and passively in a hypoacetylated form by necrotic cells, while it is known not to be released by apoptotic or secondary necrotic cells (Scaffidi *et al*., 2002). Anti-HMGB1 antibodies inhibit the inflammatory response associated with APAP hepatotoxicity and endotoxin lethality *in vivo* (Scaffidi *et al*., 2002; Wang *et al*., 1999). Increases in serum levels of HMGB1 correlate with increased mortality during endotoxin exposure *in vivo* (Wang *et al*., 1999).

Measurement of HMGB1 and K18 molecular forms provide robust end points for the mechanistic determination of cell death in a disease process. This information would be invaluable in determining the mechanistic basis of tissue damage and provide potential strategies for the therapeutic intervention of ADRs. This information would be particularly invaluable considering the multistep and multicellular nature of APAP hepatotoxicity: from bioactivation (Dahlin *et al*., 1984) to induction of cell defense (Goldring *et al*., 2004) and activation of the innate immune system (Liu *et al*., 2004).

Using a mouse model of APAP-induced hepatotoxicity, the objectives of this investigation was to use a combined molecular, proteomic, and histological approach to investigate the utility of measuring differing circulating molecular forms of HMGB1 and K18 as potential serum-based proteins to define the multidimensional mechanistic aspects of the dynamics between apoptosis, necrosis, and inflammation during DILI.

MATERIALS AND METHODS

Antibodies to HMGB1 and K18 (rabbit antihuman) were purchased from Abcam (Cambridge, UK) and antibodies to caspase-3 for both Western (rabbit anticaspase-3, 8G10) and immunohistological (rabbit anticleaved caspase, 5A1E) analyses were purchased from Cell Signaling (Hitchin, UK). Secondary (swine antirabbit IgG) and tertiary (rabbit peroxidase-antiperoxidase) antibodies for immunohistology were obtained from Dako Cytomation (Ely, UK). HMGB1 ELISA kit was purchased from Shino-Test Corporation (Tokyo, Japan). Infinity alanine aminotransferase (ALT) liquid reagent was purchased from Alpha Laboratories (Eastleigh, UK). Bio-Rad Protein Assay Dye Reagent was purchased from Bio-Rad Laboratories Ltd (Hemel Hempstead, UK). For protein analysis, α-cyano-4-hydroxycinnamic acid was purchased from Laser-Bio Labs (Sophia-Antipolis Cedex, France), trypsin from Promega (Southampton, UK), and ZipTips from Millipore (Consett, UK). All solvents were of liquid chromatography-mass spectrometry (LC-MS) grade and were the products of Fischer Scientific plc (Loughborough, UK). Unless otherwise stated, all other chemicals, peptide standards, and materials were purchased from Sigma-Aldrich (Poole, UK).

Experimental animal treatment. The protocols described were undertaken in accordance with criteria outlined in a license granted under the Animals (Scientific Procedures) Act 1986 and approved by the University of Liverpool Animal Ethics Committee. Groups of six individual male CD-1 mice (25–35 g) with free access to food and water were included in the study. For the time course, study animals were administered a single ip injection of APAP (530 mg/kg) in 0.9% saline and were euthanized 3, 5, 10, 15, 20, or 24 h after treatment. Control animals received either 0.9% saline or solvent control in 0.9% saline as appropriate. As a negative control for apoptosis and to verify apoptotic serum biomarkers as being caspase dependent, one group of mice received the pan-caspase inhibitor N-benzyloxycarbonyl-Val-Ala-Asp(OMe) fluoromethyl ketone (Z-VAD.fmk) (10 mg/kg iv in dimethyl sulfoxide [DMSO] [0.1 ml/kg DMSO in 0.9% saline] 15 min pre-APAP dose) and was euthanized 5 h after treatment. Serum ALT activity, HMGB1, and K18 levels were determined, and DNA laddering, caspase-3 Western blotting, GSH content assessment, histology, and immunohistology were performed on the livers of all animals.

Hepatotoxicity assessment. Animals were euthanized by CO_2 inhalation and cervical dislocation and blood was collected by cardiac puncture. Blood samples were stored at 4°C and allowed to clot overnight. Livers were removed and rinsed in ice-cold saline. Tissue samples were fixed in 10% neutral buffered formalin or snap frozen. Serum ALT levels were determined as previously reported (Goldring *et al*., 2004). For histological assessment of hepatotoxicity and immunohistological examination, formalin-fixed liver sections from the left lateral lobe were routinely paraffin wax embedded. Three- to five-micrometer sections were prepared and stained with hematoxylin and eosin (H&E) or used for immunohistology. H&E-stained sections were examined for any histopathological features and the identification of apoptotic and/or necrotic hepatocytes. The degree of (predominantly centrilobular) hepatocyte loss was scored 0–5, where 0 indicated no evidence of cell loss (unaltered liver) and 5 indicated extensive cell losses. The latter was performed blindly and independently by a veterinary pathologist (A.K.) and another coauthor (D.J.A.). Detailed descriptions of the histological scoring system used is presented in Supplementary Table 1. All remaining organs were also collected and evaluated for evidence of toxicity by H&E.

Determination of hepatic GSH levels. Total hepatic glutathione (GSH + oxidized glutathione) levels were determined as described previously (Williams *et al*., 2007).

Caspase-3 Western blotting, immunohistological demonstration of cleaved caspase-3, and DNA laddering. Caspase-3 Western blotting was carried out as described previously (Mercer *et al*., 2007) on mouse liver cytosol fractions prepared from snap-frozen livers. DNA was isolated from

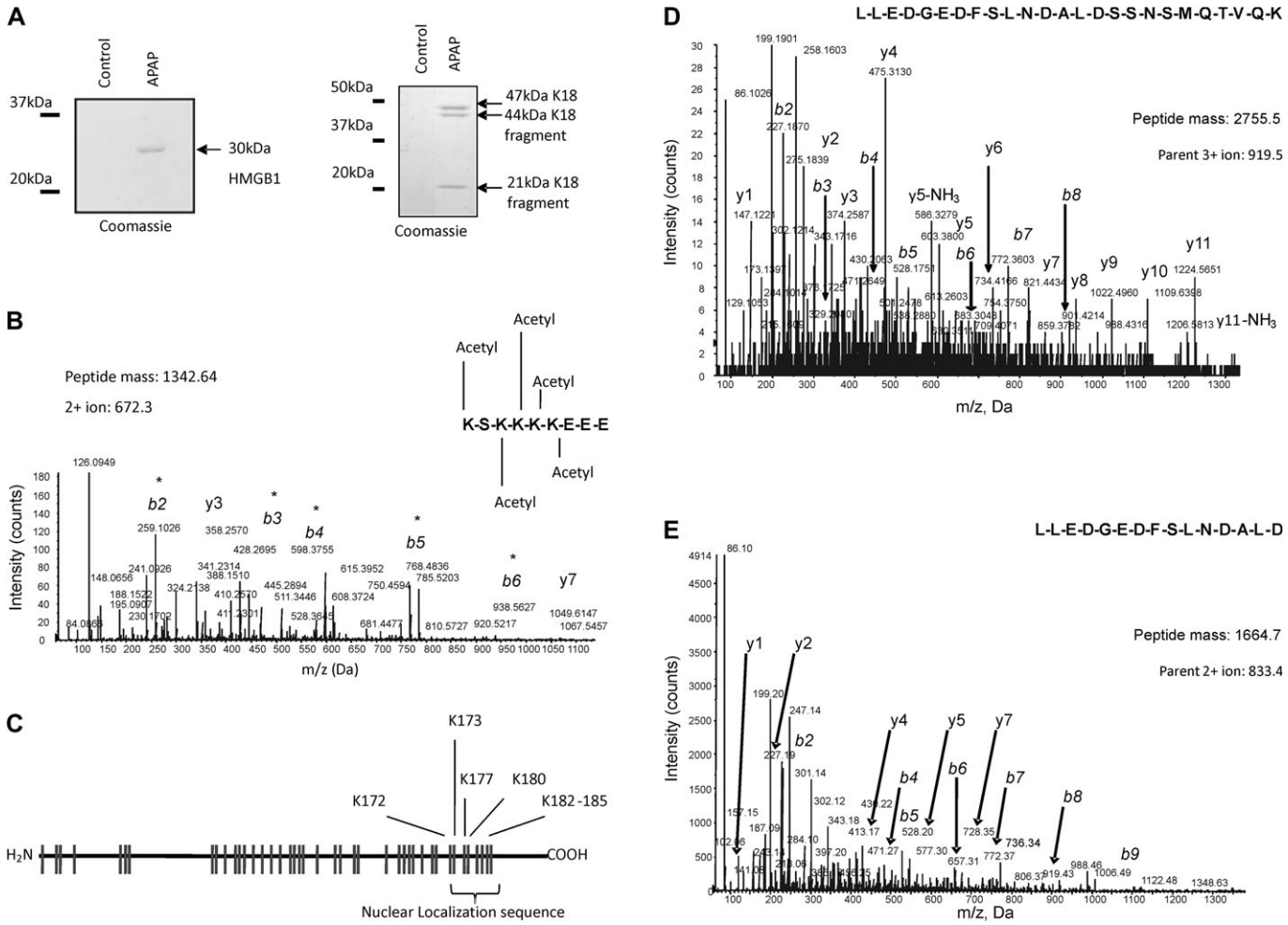

FIG. 1. Characterization of HMGB1 and K18 in the sera of mice-dosed APAP (530 mg/kg, 5 h) or 0.9% saline. (A) Coomassie blue–stained SDS-polyacrylamide gel electrophoresis gels of HMGB1 and K18 forms isolated by immunoprecipitation. (B) MS/MS analysis of murine HMGB1 peptide 180–188 acetylated on lysine residues 180 and 182–185. (C) Schematic overview of lysines within murine HMGB1 with acetylated residues identified by MS/MS within the nuclear localization sequence. (D) MS/MS characterization of peptide 375–399 from 47-kDa full-length K18 with an intact caspase cleavage motif. (E) MS/MS characterization of peptide 375–389 from caspase-cleaved K18. Figures are representative of six animals per group.

snap-frozen livers using the Sigma-Aldrich GeneElute kit according to the manufacturer's instructions. DNA laddering was visualized through ethidium bromide staining following separation on a 1% agarose gel. For the immunohistological demonstration of cleaved caspase-3, the peroxidase-antiperoxidase method was applied to formalin-fixed paraffin-embedded liver sections, based on previously described protocols (Jakob *et al*., 2008). The number of cleaved caspase-3-positive cells (cytoplasmic staining) was evaluated semiquantitatively (− no positive cells; + scattered positive cells; ++ moderate number of positive cells, and +++ numerous positive cells).

Serum HMGB1 and K18 characterization and quantification. Overnight immunoprecipitations of serum K18 and HMGB1 (5 μg antibody and protein G separation) were subjected to SDS-polyacrylamide gel electrophoresis. Protein bands were excised from Coomassie blue–stained gels and destained by incubation with 50% acetonitrile/50mM ammonium bicarbonate followed by vacuum drying. Gel pieces were rehydrated in 50mM ammonium bicarbonate containing 40 ng/μl modified trypsin (K18) or endoproteinase (GluC) (HMGB1) and incubated for 16 h at 37°C. Peptides were extracted by incubation with two changes of 60% acetonitrile/1% trifluoroacetic acid and the resulting supernatants dried. Extracts were desalted using C18 ZipTips according to the manufacturer's instructions and reconstituted in 5% acetonitrile/0.1% trifluoroacetic acid. For LC-MS/MS analysis, samples were delivered into a QSTAR Pulsar i hybrid mass spectrometer (Applied Biosystems, Foster City, CA) by automated in-line liquid chromatography (integrated LC-Packings System, 5 mm C18 nano-precolumn, and 75 μm × 15 cm C18 PepMap column [Dionex, CA]) via a nano-electrospray source head and 10-μm inner diameter PicoTip (New Objective, Woburn, MA). A gradient from 5% acetonitrile/0.05% trifluoroacetic acid (vol/vol) to 48% acetonitrile/0.05% trifluoroacetic acid (vol/vol) in 60 min was applied at a flow rate of 300 nl/min. Mass spectrometry (MS) and tandem mass spectrometry (MS/MS) spectra were acquired automatically in positive ion mode using information-dependent acquisition (Analyst; Applied Biosystems). Database searching was performed using ProteinPilot 2 (Applied Biosystems) with the latest version of the SwissProt database, with the confidence level set at 80%, and with biological modifications allowed. HMGB1 and K18 peptide analysis yielded more than 75% sequence coverage. Quantification of murine serum full-length K18 and caspase-dependent K18 fragments was accomplished through construction of standard curves generated with synthetic peptide standards spiked into a digest of an unrelated protein: The extracted ion counts for the full-length and truncated peptide were normalized for total ion count and plotted against concentration. Standards

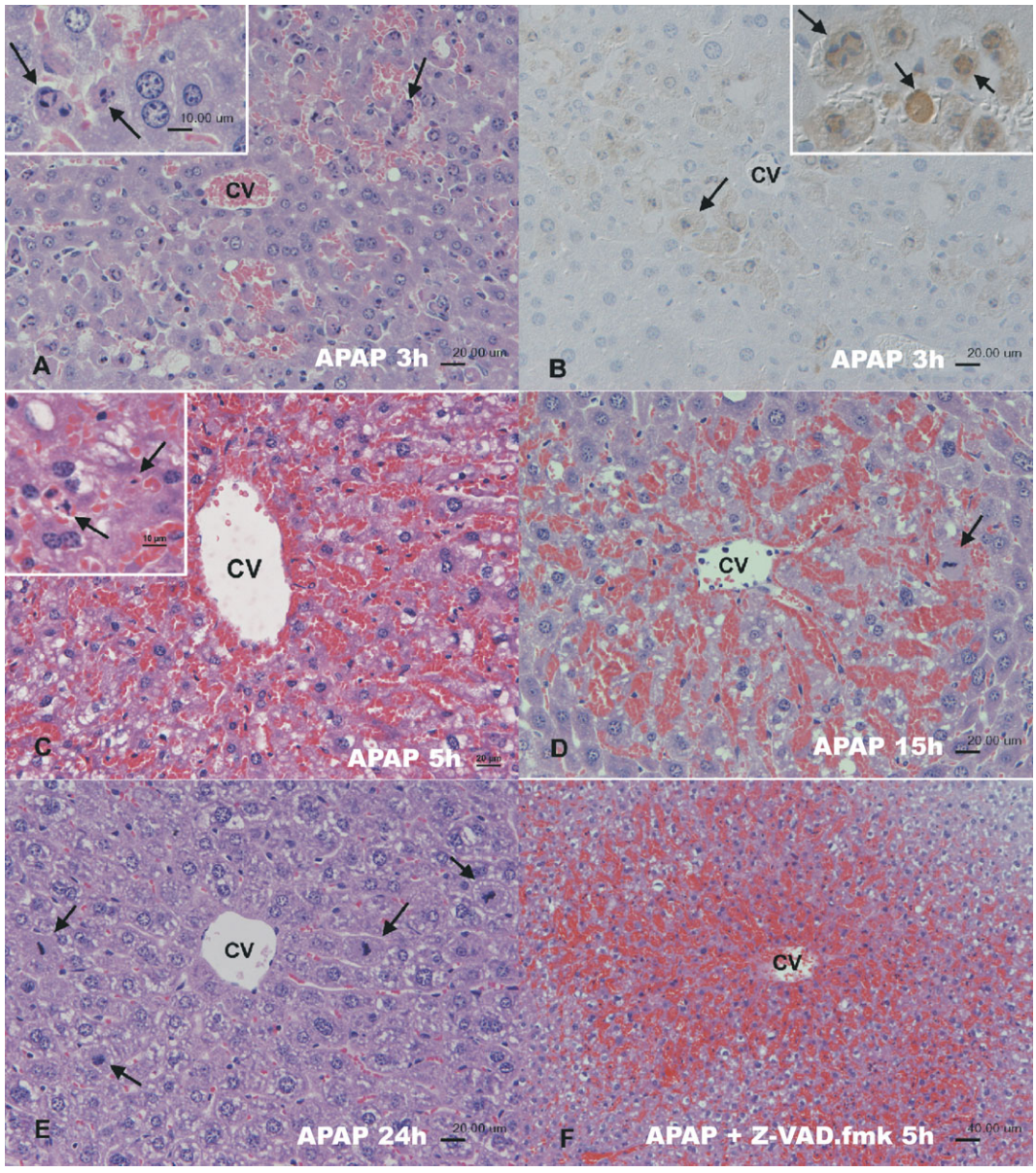

FIG. 2. Hepatic histological changes induced by APAP (530 mg/kg). (A and B) Three-hour posttreatment. There is mild centrilobular cells loss (scores 0–1). (A) Several hepatocytes exhibit morphological features of apoptosis (arrows, inset). (B) Immunohistological staining for cleaved caspase-3 confirms these cells as apoptotic (arrows; inset). (A) H&E stain. (B) Peroxidase-antiperoxidase method, Papanicolaou's hematoxylin counterstain. Bar = 20 µm. (C) Five-hour posttreatment. Extensive centrilobular cell loss (individual animal score 2, group average 2.2) is seen. Inset, there are scattered necrotic cells but apoptotic cells are not observed. H&E stain. Bar = 20 µm. (D) Fifteen-hour posttreatment. Extensive centrilobular cell loss (score 2) is present, but there is evidence of hepatocyte replacement. Arrow, hepatocyte undergoing mitosis. H&E stain. Bar = 20 µm. (E) Twenty-four-hour posttreatment. There is no evidence of hepatocyte loss (score 0) and several mitotic hepatocytes are seen (arrows). H&E stain. Bar = 20 µm. (F) Five-hour post-APAP + Z-VAD.fmk treatment. There is extensive centrilobular hepatocyte loss (individual animal score 3, group average 3.4) without evidence of apoptosis. H&E stain. Bar =10 µm. CV, central vein. Figures are representative of six animals per group. A–E ×20 magnification. Inserts are ×40 magnification. F ×10 magnification.

were spiked into and could be recovered from control serum. The full-length K18 standard (LLEDGEDFSLNDALDSSNSMQTVQK) was designed to span the caspase-3, -7, and -9 cleavage site, whereas the abbreviated peptide (LLEDGEDFSLNDALD) was derived from K18 fragments following caspase cleavage. Necrosis related HMGB1 and the hyper-acetylated derivative were also quantified using the normalized extracted ion counts of the peptide peak. Since no synthetic standards were available, values are presented as relative values and compared to total levels of serum HMGB1 determined by ELISA according to the manufacturer's instructions. Assay validation data are available as Supplementary Table 2.

Statistical analysis. All results (excluding histological and immunohistological analysis) are expressed as mean ± SD. Values to be compared were analyzed for nonnormality using a Shapiro-Wilk test. The unpaired *t*-test was used when normality was indicated. A Mann-Whitney *U*-test was used for nonparametric data. All calculations were performed using StatsDirect statistical software; results were considered to be significant when $p < 0.05$.

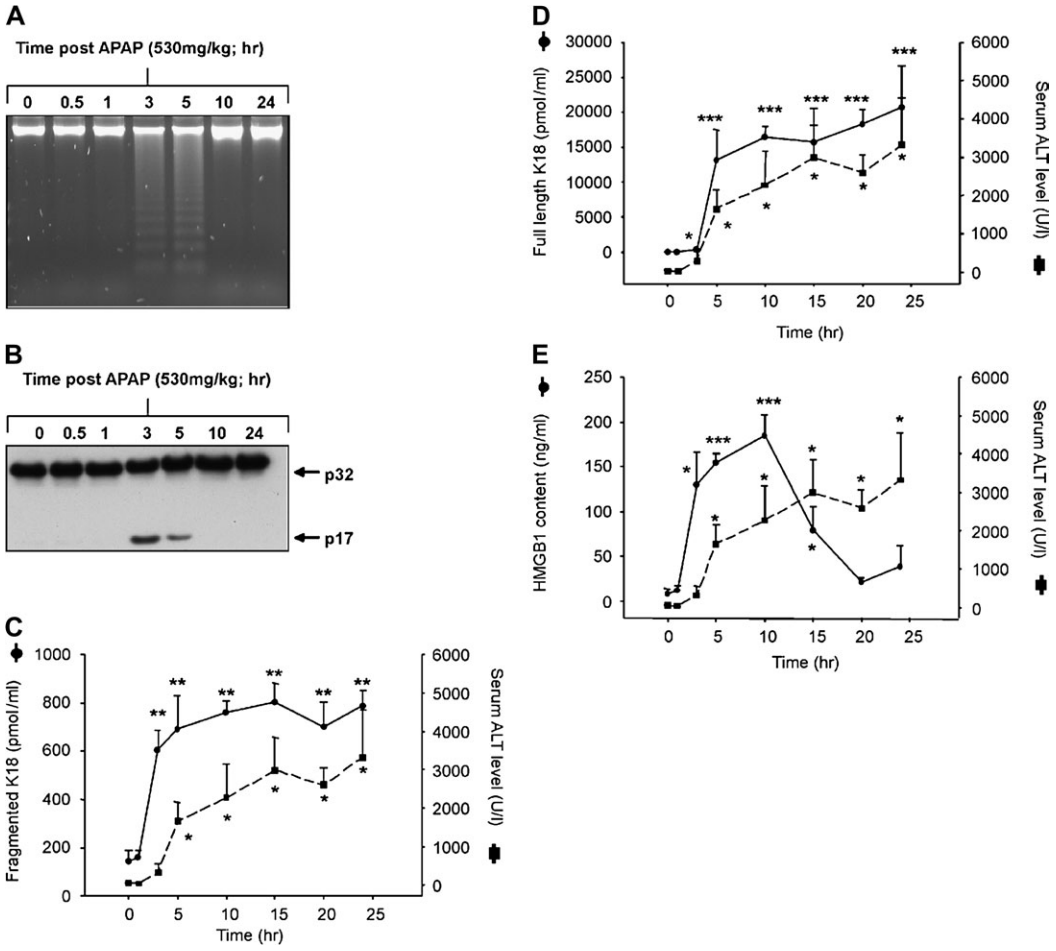

FIG. 3. Time-course evaluation following APAP administration (530 mg/kg, 0–24 h) of (A) hepatic DNA laddering determined by agarose gel analysis, (B) processing of hepatic procaspase-3 (p32) to the active fragment (p17) determined by Western blot. Simultaneous time-course correlation of ALT activity (dotted line, unit per liter) with (C) caspase-cleaved K18 fragment level (solid line, picomole per milliliter), (D) full-length K18 level (solid line, picomole per milliliter), and (E) total HMGB1 level (solid line, nanogram per milliliter) present in the serum of APAP-dosed mice. Figures are representative of six animals per group. Data given as mean ± SD. Statistical significance was assigned relative to vehicle-treated controls from the same time point as defined in ''Materials and Methods section.'' $*p < 0.05$, $**p < 0.01$, and $***p < 0.005$.

RESULTS

Caspase-Cleaved K18, Full-Length K18, Hypoacetylated HMGB1, and Hyperacetylated HMGB1 are Present in Mouse Serum during APAP-Induced Hepatotoxicity

LC-MS/MS characterization of the GluC-digested 30-kDa protein revealed only the isolation of HMGB1 from the sera of APAP-dosed mice but not present in control (Fig. 1A). MS/MS analysis confirmed a mixture of both hypoacetylated (released by necrotic cells) and hyperacetylated (released from activated immune cells) HMGB1. A peptide of 1132.6 Da was identified containing lysine residues 180 and 182–185 (GluC peptide KSKKKKEEE) derived from the HMGB1 nuclear localization sequence. Another peptide was also present with the same amino acid sequence but had a mass increase of 210 amu. The increase in mass to 1342.6 Da corresponded to the addition of five acetyl groups. Further MS/MS analysis confirmed the acetylation modifications to be present on lysine residues 180 and 182–185 (Figs. 1B and 1C), which is known to be a key mechanism for the active release of the protein by monocytes and macrophages (Bonaldi *et al*., 2003).

Characterization of K18 present in the sera of APAP-dosed mice resulted in the identification of the full-length K18 (47 kDa, known to be released from necrotic cells) and two apoptosis-related forms at 44 and 21 kDa (Fig. 1A). In the sera of untreated mice, no evidence was found for release of the full-length or fragmented forms of K18 (Fig. 1A). MS analysis of the tryptic digest of full-length K18 yielded a 2756-Da peptide (^{375}LLEDGEDFSLNDALDSSNSMQTVQK^{399}) that is not present in digests of the caspase-cleaved apoptotic fragments of K18 (44 and 21 kDa). This peptide was shown to possess the intact predicted caspase-3, -7, and -9 cleavage motif (Fig. 1D). Tryptic digestion of the 44- and 21-kDa K18 fragments yielded a foreshortened peptide of 1665 Da

TABLE 1
Time-Course Evaluation of Hepatic Histological and Serum Biomarker Changes Induced by Acute APAP Administration to the CD-1 Mouse

Time point (h)	Main histological features	Cell loss score (average)	*In situ* cleaved caspase-3 (IH)	GSH depletion	DNA ladder	Caspase-3 processing (WB)	Serum biomarker elevation			
							K18 (fragment)	K18 (full length)	Total HMGB1	ALT
3	Centrilobular cell loss—numerous apoptotic cells.	1–2	+++	+	+	+	+	+	+	+
5	Centrilobular cell loss and space filled by erythrocytes, variable numbers of apoptotic cells, and increased number of necrotic cells, mainly centrilobular; increased numbers of mitotic hepatocytes, mild centrilobular neutrophil infiltration.	1–3 (2)	−/+/++/+++	+	−/+	−/+	−/+	+	+	+
10	Centrilobular cell loss and space filled by erythrocytes, no or only scattered apoptotic cells, mainly centrilobular; increased numbers of mitotic hepatocytes, mild centrilobular neutrophil infiltration.	1–2	−/+	−	−	+	+	+	+	+
15	Centrilobular cell loss but evidence of centrilobular cell replacement; numerous mitotic hepatocytes, mild centrilobular neutrophil infiltration.	0–2 (1/2)	−	−	−	−	+	+	+	+
20	No evidence of or mild centrilobular cell loss; irregularly arranged centrilobular hepatocytes; numerous mitotic hepatocytes.	0–1	−	−	−	−	+	+	−	+
24	No evidence of centrilobular hepatocyte loss; numerous mitotic hepatocytes.	0	−	−	−	−	+	+	−	+

Note. IH, immunohistology; WB, Western blot.

Summary of histological changes, induction of apoptotic biomarkers (caspase-3 activation and DNA laddering), and serum biomarker evaluation induced by APAP in male CD-1 mice (530 mg/kg) over 3–24 h. For IH, −, +, ++, and +++ indicates the degree of hepatic-cleaved caspase-3 (as described in ''Materials and Methods section''). For GSH depletion, + indicates significant or − indicates nonsignificant hepatic GSH depletion compared to control animals. For DNA laddering and the demonstration of caspase-3 processing by WB, + indicates a positive result. For serum biomarker analysis, + indicates a significant elevation above control values or − indicates no significant increase above control values. The results are representative of six animals per group.

(^{375}LLEDGEDFSLNDALD^{389}) absent from the full-length K18. MS analysis revealed that this was due to the presence of the caspase site being cleaved at the DALD/SS motif (Fig. 1E).

K18 and HMGB1 Represent Sensitive and Informative Mechanism-Based Biomarkers of APAP-Induced Histological Changes

During the time course investigation of the acute toxicity associated with APAP, the liver was the only organ affected by APAP. Individual animal time-course data are available as Supplementary material, which provides evidence of significant elevations in K18 or HMGB1 levels when histology scores are increased despite no significant elevation in serum ALT activity (Supplementary Table 3). Control animals did not show any histological or immunohistological changes (score 0). At 3-h posttreatment, centrilobular cell loss (mean: 1.2) was observed and there were numerous apoptotic cells in the centrilobular region (Fig. 2A). Apoptosis of these cells was confirmed by their expression of cleaved caspase-3 (Fig. 2B) and further by DNA laddering, procaspase-3 processing, and serum K18 fragment elevation (Figs. 3A and 3B). At 5-h posttreatment, animals exhibit a variable degree of cell loss (Table 1, mean: 2.3). Livers with a score of 1 exhibited numerous apoptotic cells and were thereby generally similar to those described for 3-h posttreatment, indicating a possible delayed onset of toxic effects in some animals. In livers with a score of 2 or 3, however, apoptotic cells were very rare and occasional necrotic cells were seen (Fig. 2C). When apoptotic cells were not identified *in situ*, DNA laddering and/or caspase-3 processing was not observed either. By 10-h posttreatment, cell loss was scored 1 or 2 and apoptotic or necrotic cells were rare. There was no evidence of DNA laddering and caspase-3 processing; however, serum K18 fragment elevation was still observed. At 15-h posttreatment, serum K18 fragments were still elevated. Mean hepatocyte loss was scored 1.2 and there was evidence of centrilobular hepatocyte replacement (Fig. 2D). At 20-h posttreatment, there was minimal hepatocyte loss (score 0 or 1) and centrilobular hepatocytes appeared irregularly arranged. This irregularity was no longer apparent at

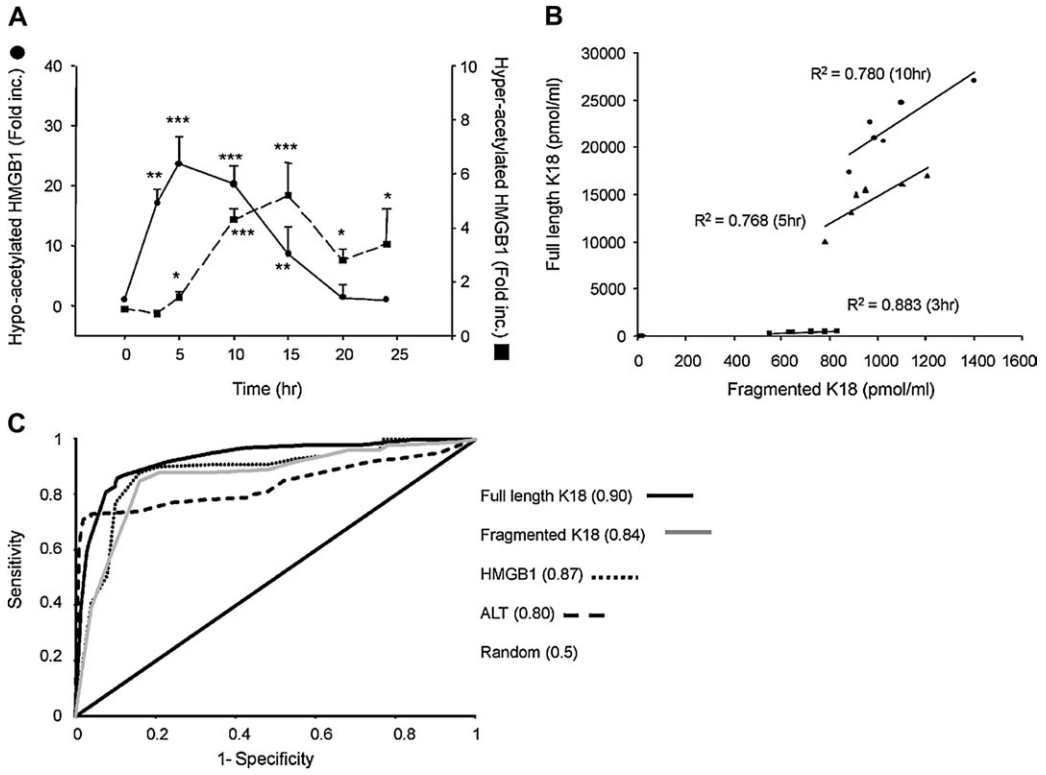

FIG. 4. (A) Fold increase in serum hyperacetylated (immune cell derived, dotted line) and hypoacetylated (released by necrotic cells, solid line) HMGB1 over 0–24 h and (B) correlation of serum caspase–cleaved K18 as a marker of apoptosis against full-length K18 as a marker of necrosis in individual mice over 10 h following APAP administration (530 mg/kg), correlation coefficients given when required. (C) ROC analysis indicating sensitivity and specificity of serum K18, fragmented K18, HMGB1, and ALT as biomarkers of APAP hepatotoxicity in the mouse. Data are given as mean ± SD of six mice per group. Statistical significance was assigned relative to time-matched vehicle-dosed controls. $*p < 0.05$, $**p < 0.01$, and $***p < 0.005$.

24-h posttreatment when all livers were scored 0 (Fig. 2E). From 5-h posttreatment, there was evidence of increased hepatocyte mitosis, represented by mitotic figures, which were numerous at 15-, 20-, and 24-h posttreatment (Figs. 2D and 2E). Serum full-length K18 elevation and increased serum ALT activity were observed over the entire time course (Fig. 3D), while serum HMGB1 elevation was not seen beyond 10-h posttreatment (Fig. 3E) and GSH depletion was only obvious 3- and 5-h posttreatment. Between 5 and 15 h, small numbers of neutrophils were seen centrilobularly in some animals (Table 1). The variation in the level of full-length versus caspase-cleaved K18 present in serum following APAP administration shows the change from mixed apoptotic/necrotic to necrotic cell death over time (Fig. 4B). In all cases, the serum elevation in either HMGB1 or K18 was observed at time points earlier than ALT activity (Figs. 3C–E).

Following APAP administration, MS/MS analysis of the serum hypoacetylated and hyperacetylated forms of HMGB1 revealed a significant elevation in the necrosis-associated form at 3-h postdose, which peaked at 5 h and returned to control levels by 20 h. In contrast, the serum level of the immune cell derived form of HMGB1 was first significantly elevated above control levels at 5-h postdose. It then increased further, peaked at 15 h, and was still significantly elevated by 24 h (Fig. 4A). Receiver operator characteristic (ROC) analysis was undertaken for HMGB1 and K18 (full length and fragmented) in comparison with ALT. Figure 4C demonstrates ROC curves and area under the curve analysis for serum fragmented K18 (0.84), full-length K18 (0.90), and total HMGB1 (0.87) compared to ALT (0.80). Further verification of HMGB1 and K18 as biomarkers of DILI was assessed by correlating individual animal serum HMGB1 and K18 levels with the degree of hepatocyte loss determined by histology at 5 h (Figs. 5A and 5B). Increases in both serum full-length K18 and HMGB1 correlated with an increase in the degree of hepatocyte loss. Correlation coefficients of $R^2 = 0.832$ and $R^2 = 0.746$ were obtained for K18 and HMGB1, respectively, when correlated with the level of ALT activity following APAP administration (Figs. 5C and 5D).

Caspase Inhibition Increases APAP-Induced Necrosis

At 5-h posttreatment with APAP and Z-VAD.fmk, apoptotic markers were not detected in any of these animals (Figs. 6A–C), whereas the degree of GSH depletion was not affected (Fig. 6D). Serum ALT and serum HMGB1 levels were higher than with APAP administration alone (Figs. 6E and 6F). The degree of centrilobular hepatocyte loss was significantly higher (Fig. 2F).

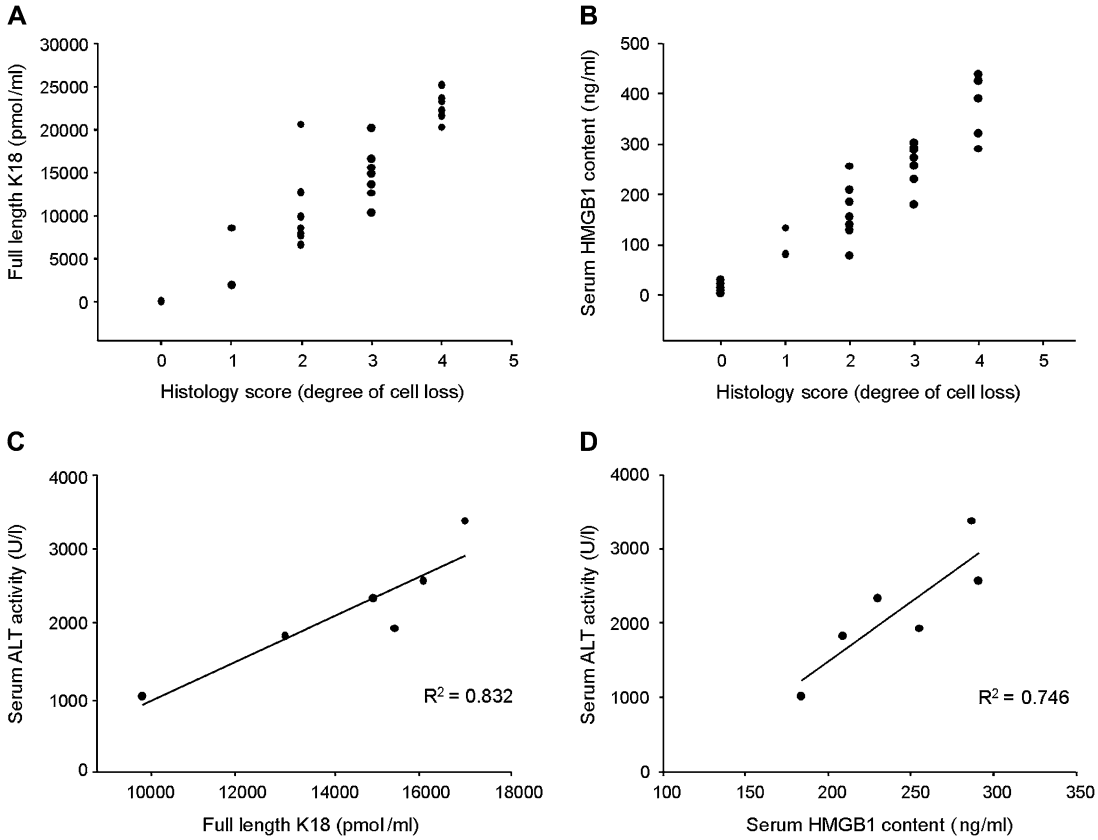

FIG. 5. Correlation of individual animal serum (A) full-length K18 level (picomole per milliliter) and (B) total HMGB1 content (nanogram per milliliter) with the degree of cell loss (histology score). Correlation of individual animal serum ALT activity (unit per liter) with (C) full-length K18 level and (D) total HMGB1 content. Correlation coefficients indicated were required. Mice received 0.9% saline, APAP 530 mg/kg or APAP 530 mg/kg, and Z-VAD.fmk 10 mg/kg for 5 h.

DISCUSSION

We have combined a mass spectrometric, histological, and proteomic evaluation to investigate the use of differing circulating molecular forms of HMGB1 and K18 in a murine model of APAP-induced hepatotoxicity. We report the quantification of the dynamics of circulating HMGB1 and K18 molecular forms that provide a sensitive- and mechanism-based indicator of the pathological changes observed within inaccessible tissues. This particularly reflects the multistep process and multiple cell types involved during the onset of APAP-induced liver injury through to recovery.

Hepatocyte apoptosis was induced by APAP in the early phase after treatment (3–5 h). This occurred alongside the induction of necrosis, which is the only form of cell death observed at later time points by histology (10–15 h). Characterization of K18 by MS/MS identified both full-length K18, released passively by necrosis, and fragmented K18, released during apoptosis (Tao *et al*., 2008), in the sera of mice that had received toxic doses of APAP. MS/MS confirmed that in the fragmented forms of K18 (DALD), but not the full-length form (DALDSS), the protein was cleaved by caspases at the consensus motif and in a time-dependent manner. Caspase cleavage of K18 strongly correlated with the demonstration of procaspase processing, DNA laddering, and the presence of morphologically apoptotic hepatocytes that express cleaved caspase-3 *in situ*. Moreover, MS analysis permitted accurate analyte identification and the simultaneous analysis of elevations in the apoptosis- and necrosis-related K18 forms within the same sample.

Correlations between full-length and caspase-cleaved K18 levels by MS in individual animals provided a serum-based method to demonstrate the change from mixed apoptotic/necrotic cell death within the first few hours posttreatment (3–5 h) to necrosis only at later time points. The cell death–specific forms of K18 correlated strongly with histological features, which indicated a progression or a switch from apoptosis to necrosis in the early phase of APAP hepatotoxicity (3- to 5-h posttreatment). K18 quantification confirmed that necrosis was the major form of cell death at late time points. Histologically, the presence of apoptotic cells at earlier time points could easily be confirmed, as cells with the typical morphological changes that expressed cleaved caspase-3 were demonstrated. Necrotic cells, however, were rarely identified histologically. This confirms that hepatocyte necrosis, when compared to apoptosis, is a very rapid process, which leads to almost instant

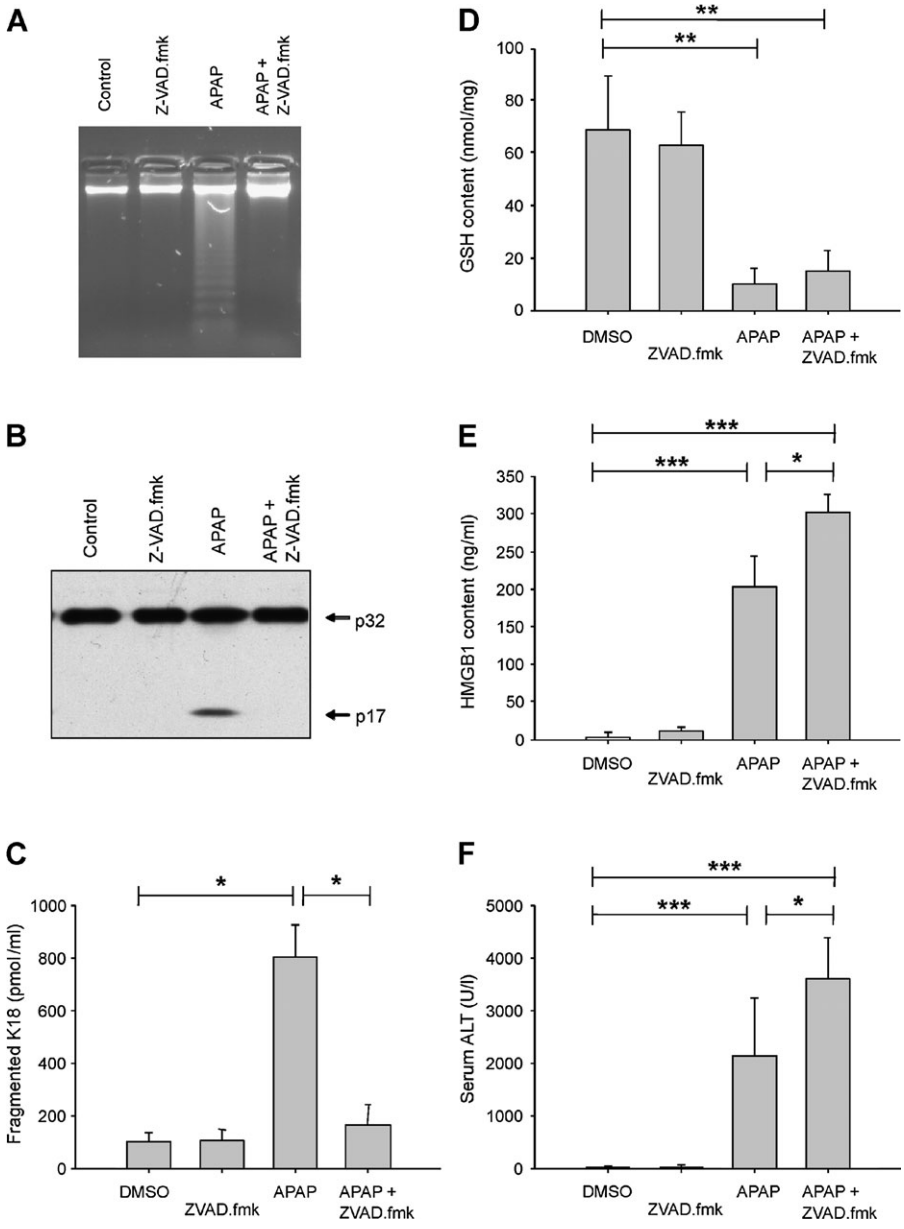

FIG. 6. Effect of caspase inhibition via Z-VAD.fmk on APAP (530 mg/kg; 5 h) hepatotoxicity. (A) Hepatic DNA laddering, (B) procaspase-3 processing, (C) serum caspase–cleaved K18 abundance (picomole per milliliter), (D) hepatic GSH depletion (nanomole per milligram), (E) total serum HMGB1 content (nanogram per milliliter), and (F) serum ALT activity (unit per liter) recorded simultaneously within the same group of mice. Data are representative of mean ± SD of six mice per group. Statistical significance was assigned relative to time-matched vehicle-dosed controls. *$p < 0.05$, **$p < 0.01$, and ***$p < 0.005$.

cell loss from the liver parenchyma via the blood (Green, 2005).

APAP-induced cleavage of K18 resulted in both a large 44-kDa fragment being produced through cleavage by caspases-3, -7, and -9 and a smaller K18 fragment dependent upon the additional activity of caspase-6. This information could not be derived from current immunoassays, which do not differentiate between the 44- and 21-kDa fragments. However, a 27-kDa fragment derived from caspase-6 cleavage alone could not be identified (Tao *et al*., 2008). The incomplete cleavage of K18 could result from the rapid depletion of hepatic ATP during APAP hepatotoxicity. The importance of APAP-induced apoptosis to the resulting level of liver injury was further demonstrated by the results of the time course and caspase inhibition investigation. The induction of cell death and subsequent activation of mitosis lead to organ regeneration in this mouse model. Enhanced hepatic necrosis was seen with the caspase-inhibited mice treated with APAP, as shown by an increase in serum necrosis–related HMGB1, ALT activity, and histological analysis compared to APAP alone. This evidence

suggests that a shift in the cell death dynamics may serve as a protective mechanism to halt the speed and spread of liver damage and to avoid a systemic inflammatory response by inhibiting the release of proinflammatory agents such as HMGB1. However, further investigations looking at an extended time course following Z-VAD.fmk cotreatment and the assessment of liver failure will be required to confirm this. The molecular forms of HMGB1 and K18 present in the sera of mice could be used to identify the tipping point between the activation of apoptosis and necrosis in an inaccessible tissue; however, further investigation is required to explain the significance of this to the overall extent of injury manifestation. As seen *in vitro*, the possibility exists that inhibition of caspase activity sensitizes hepatocytes to necrosis in a mechanism related to the enhanced production of reactive oxygen intermediates. Also, the insufficient removal of damaged mitochondria seen with Z-VAD.fmk sensitization to tumor necrosis factor–induced cytotoxicity may play a role (Vercammen *et al*., 1998). This requires further investigation in this mouse model of APAP hepatotoxicity.

MS/MS analysis also identified both hypoacetylated HMGB1, which is released from necrotic cells (Scaffidi *et al*., 2002), and hyperacetylated HMGB1, which is derived from activated immune cells (Bonaldi *et al*., 2003), in the sera of APAP-treated mice. Currently available commercial immunoassays do not distinguish between the various molecular forms of HMGB1. Moreover, MS/MS analysis identified the acetylation of key lysine residues 180 and 182–185 within the nuclear localization sequence, which has previously been identified as critical for the immune cell release of HMGB1 (Bonaldi *et al*., 2003). During APAP hepatotoxicity, the level of the molecular form of HMGB1 derived from necrosis was significantly increased from 3-h posttreatment, peaked at 10 h, then decreased, and was not detectable at 20 h. Interestingly, by 15-h posttreatment, there was no histological evidence of further hepatocyte necrosis, yet there was evidence of liver regeneration based on the more abundant presence of mitotic hepatocytes as early as 5-h posttreatment. The fact that HMGB1 has a relatively short half-life in serum and that its elevation and subsequent decrease mirrored the short-time scale of actual hepatic cell loss highlights the importance of HMGB1 protein as a blood-based reflective indicator of pathological changes within inaccessible tissues. In contrast, the immune cell derived form of HMGB1 was increased from 5 h until the end of the experiment at 24 h but to a much lesser extent. Interestingly, only small numbers of neutrophils were seen centrilobularly in some animals between 5- and 15-h post-APAP, a finding that mirrors the changes in acute APAP hepatotoxicity described in humans (Davidson and Eastham, 1966). This indicates that necrotic hepatocyte death induced by APAP leads to systemic immune cell activation but not necessarily influx of inflammatory cells into the damaged liver. ROC curve analysis of the time course of APAP treatment supported the observation that K18 and HMGB1 were sensitive and specific indicators of hepatotoxicity; although as predicted, ALT analysis was a more organ-specific marker of hepatic damage. Further verification of K18 and HMGB1 as mechanism-based indices of APAP hepatotoxicity was achieved by revealing the strong correlations between serum levels and both *in situ* cell loss and ALT activity at the maximum level of liver injury assessed by histology as well as the disappearance of the apoptotic biomarkers in the sera of the caspase inhibition model.

This report demonstrates the novel MS characterization and identification of circulating HMGB1 and K18 in the investigation of liver injury in a mouse model of DILI. HMGB1 and K18 were informative serum proteins of the pathological changes induced within tissues by APAP. These proteins are related to the documented mechanisms of APAP-induced liver injury (apoptosis, necrosis, and inflammation). These proteins can now be used to investigate structure-metabolism relationships and structure-toxicity relationships for other hepatotoxins, especially considering the step dose-response curves and rapid transition between apoptotic and necrotic cell death observed within this murine model. Further qualification investigations are required to determine their utility for investigating mechanisms of DILI in man. Nevertheless, such functional serum biomarkers have potential to be used in bridging studies between *in vitro*, preclinical, and clinical models in research to enhance our mechanistic understanding of DILI as well as tools for the noninvasive fundamental mechanistic investigation of cell death dynamics *in vivo*.

SUPPLEMENTARY DATA

Supplementary data are available online at http://toxsci.oxfordjournals.org/.

FUNDING

Medical Research Council to (D.J.A).

ACKNOWLEDGMENTS

The authors are grateful to the Histology Laboratories, Department of Veterinary Pathology, Faculty of Veterinary Science, University of Liverpool, in particular to Ms Valerie Tilston for excellent technical support. The authors also wish to thank Dr. Martin Heinrichs (Sanofi Aventis Deutschland GmbH) for useful discussions.

REFERENCES

Bantel, H., Lugering, A., Heidemann, J., Volkmann, X., Poremba, C., Strassburg, C. P., Manns, M. P., and Schulze-Osthoff, K. (2004). Detection of apoptotic caspase activation in sera from patients with chronic HCV infection is associated with fibrotic liver injury. *Hepatology* **40,** 1078–1087.

Bonaldi, T., Talamo, F., Scaffidi, P., Ferrera, D., Porto, A., Bachi, A., Rubartelli, A., Agresti, A., and Bianchi, M. E. (2003). Monocytic cells hyperacetylate chromatin protein HMGB1 to redirect it towards secretion. *EMBO J.* **22,** 5551–5560.

Caulin, C., Salvesen, G. S., and Oshima, R. G. (1997). Caspase cleavage of keratin 18 and reorganization of intermediate filaments during epithelial cell apoptosis. *J. Cell Biol.* **138,** 1379–1394.

Cummings, J., Hodgkinson, C., Odedra, R., Sini, P., Heaton, S. P., Mundt, K. E., Ward, T. H., Wilkinson, R. W., Growcott, J., Hughes, A., *et al*. (2008a). Preclinical evaluation of M30 and M65 ELISAs as biomarkers of drug induced tumor cell death and antitumor activity. *Mol. Cancer Ther.* **7,** 455–463.

Cummings, J., Ward, T. H., Greystoke, A., Ranson, M., and Dive, C. (2008b). Biomarker method validation in anticancer drug development. *Br. J. Pharmacol.* **153,** 646–656.

Dahlin, D. C., Miwa, G. T., Lu, A. Y., and Nelson, S. D. (1984). N-acetyl-p-benzoquinone imine: a cytochrome P-450-mediated oxidation product of acetaminophen. *Proc. Natl. Acad. Sci. U.S.A.* **81,** 1327–1331.

Davidson, D. G., and Eastham, W. N. (1966). Acute liver necrosis following overdose of paracetamol. *BMJ* **2,** 497–499.

Goldring, C. E., Kitteringham, N. R., Elsby, R., Randle, L. E., Clement, Y. N., Williams, D. P., McMahon, M., Hayes, J. D., Itoh, K., Yamamoto, M., *et al*. (2004). Activation of hepatic Nrf2 in vivo by acetaminophen in CD-1 mice. *Hepatology* **39,** 1267–1276.

Green, D. R. (2005). Apoptotic pathways: ten minutes to dead. *Cell* **121,** 671–674.

Gujral, J. S., Knight, T. R., Farhood, A., Bajt, M. L., and Jaeschke, H. (2002). Mode of cell death after acetaminophen overdose in mice: apoptosis or oncotic necrosis? *Toxicol. Sci.* **67,** 322–328.

Gunawan, B. K., Liu, Z. X., Han, D., Hanawa, N., Gaarde, W. A., and Kaplowitz, N. (2006). c-Jun N-terminal kinase plays a major role in murine acetaminophen hepatotoxicity. *Gastroenterology* **131,** 165–178.

Hori, O., Brett, J., Slattery, T., Cao, R., Zhang, J., Chen, J. X., Nagashima, M., Lundh, E. R., Vijay, S., and Nitecki, D. (1995). The receptor for advanced glycation end products (RAGE) is a cellular binding site for amphoterin. Mediation of neurite outgrowth and co-expression of rage and amphoterin in the developing nervous system. *J. Biol. Chem.* **270,** 25752–25761.

Imaeda, A. B., Watanabe, A., Sohail, M. A., Mahmood, S., Mohamadnejad, M., Sutterwala, F. S., Flavell, R. A., and Mehal, W. Z. (2009). Acetaminophen-induced hepatotoxicity in mice is dependent on Tlr9 and the Nalp3 inflammasome. *J. Clin. Invest.* **119,** 305–314.

Jaeschke, H. (2006). How relevant are neutrophils for acetaminophen hepatotoxicity? *Hepatology* **43,** 1191–1194.

Jakob, S., Corazza, N., Diamantis, E., Kappeler, A., and Brunner, T. (2008). Detection of apoptosis in vivo using antibodies against caspase-induced neo-epitopes. *Methods* **44**(3), 255–261.

Kon, K., Ikejima, K., Okumura, K., Aoyama, T., Arai, K., Takei, Y., Lemasters, J. J., and Sato, N. (2007). Role of apoptosis in acetaminophen hepatotoxicity. *J. Gastroenterol. Hepatol.* **22**(Suppl. 1), S49–S52.

Kono, H., and Rock, K. L. (2008). How dying cells alert the immune system to danger. *Nat. Rev. Immunol.* **8,** 279–289.

Ku, N. O., and Omary, M. B. (2001). Effect of mutation and phosphorylation of type I keratins on their caspase-mediated degradation. *J. Biol. Chem.* **276,** 26792–26798.

Liu, Z. X., Govindarajan, S., and Kaplowitz, N. (2004). Innate immune system plays a critical role in determining the progression and severity of acetaminophen hepatotoxicity. *Gastroenterology* **127,** 1760–1774.

Masson, M. J., Carpenter, L. D., Graf, M. L., and Pohl, L. R. (2008). Pathogenic role of NKT and NK cells in acetaminophen-induced liver injury is dependent on the presence of DMSO. *Hepatology* **48,** 889–897.

Mercer, A. E., Maggs, J. L., Sun, X. M., Cohen, G. M., Chadwick, J., O'Neill, P. M., and Park, B. K. (2007). Evidence for the involvement of carbon-centered radicals in the induction of apoptotic cell death by artemisinin compounds. *J. Biol. Chem.* **282,** 9372–9382.

Park, B. K., Kitteringham, N. R., Maggs, J. L., Pirmohamed, M., and Williams, D. P. (2005). The role of metabolic activation in drug-induced hepatotoxicity. *Annu. Rev. Pharmacol. Toxicol.* **45,** 177–202.

Park, J. S., Svetkauskaite, D., He, Q., Kim, J. Y., Strassheim, D., Ishizaka, A., and Abraham, E. (2004). Involvement of toll-like receptors 2 and 4 in cellular activation by high mobility group box 1 protein. *J. Biol. Chem.* **279,** 7370–7377.

Pirmohamed, M., James, S., Meakin, S., Green, C., Scott, A. K., Walley, T. J., Farrar, K., Park, B. K., and Breckenridge, A. M. (2004). Adverse drug reactions as cause of admission to hospital: prospective analysis of 18820 patients. *BMJ* **329,** 15–19.

Scaffidi, P., Misteli, T., and Bianchi, M. E. (2002). Release of chromatin protein HMGB1 by necrotic cells triggers inflammation. *Nature* **418,** 191–195.

Schutte, B., Henfling, M., Kolgen, W., Bouman, M., Meex, S., Leers, M. P., Nap, M., Bjorklund, V., Bjorklund, P., Bjorklund, B., *et al*. (2004). Keratin 8/18 breakdown and reorganization during apoptosis. *Exp. Cell Res.* **297,** 11–26.

Tao, G. Z., Li, D. H., Zhou, Q., Toivola, D. M., Strnad, P., Sandesara, N., Cheung, R. C., Hong, A., and Omary, M. B. (2008). Monitoring of epithelial cell caspase activation via detection of durable keratin fragment formation. *J. Pathol.* **215,** 164–174.

Vercammen, D., Beyaert, R., Denecker, G., Goossens, V., Van Loo, G., Declercq, W., Grooten, J., Fiers, W., and Vandenabeele, P. (1998). Inhibition of caspases increases the sensitivity of L929 cells to necrosis mediated by tumor necrosis factor. *J. Exp. Med.* **187,** 1477–1485.

Wang, H., Bloom, O., Zhang, M., Vishnubhakat, J. M., Ombrellino, M., Che, J., Frazier, A., Yang, H., Ivanova, S., Borovikova, L., *et al*. (1999). HMG-1 as a late mediator of endotoxin lethality in mice. *Science* **285,** 248–251.

Wieckowska, A., Zein, N. N., Yerian, L. M., Lopez, A. R., McCullough, A. J., and Feldstein, A. E. (2006). In vivo assessment of liver cell apoptosis as a novel biomarker of disease severity in nonalcoholic fatty liver disease. *Hepatology* **44,** 27–33.

Williams, D. P., Antoine, D. J., Butler, P. J., Jones, R., Randle, L., Payne, A., Howard, M., Gardner, I., Blagg, J., and Park, B. K. (2007). The metabolism and toxicity of furosemide in the Wistar rat and CD-1 mouse: a chemical and biochemical definition of the toxicophore. *J. Pharmacol. Exp. Ther.* **322,** 1208–1220.